6-2008

Differential transcriptional analysis of the cyanobacterium Cyanothece sp. ATCC 51142 during light-dark and continuous-light growth.

Jörg Toepel

Eric Welsh

Tina C. Summerfield

Himadri B. Pakrasi

Louis A. Sherman
Purdue University, lsherman@purdue.edu

Follow this and additional works at: http://docs.lib.purdue.edu/bioscipubs

Journal of Bacteriology

Differential Transcriptional Analysis of the Cyanobacterium *Cyanothece* sp. Strain ATCC 51142 during Light-Dark and Continuous-Light Growth

Jörg Toepel, Eric Welsh, Tina C. Summerfield, Himadri B. Pakrasi and Louis A. Sherman

Updated information and services can be found at:
http://jb.asm.org/content/190/11/3904

These include:

SUPPLEMENTAL MATERIAL Supplemental material

REFERENCES This article cites 51 articles, 27 of which can be accessed free
at: http://jb.asm.org/content/190/11/3904#ref-list-1

CONTENT ALERTS Receive: RSS Feeds, eTOCs, free email alerts (when new
articles cite this article), more»

Differential Transcriptional Analysis of the Cyanobacterium *Cyanothece* sp. Strain ATCC 51142 during Light-Dark and Continuous-Light Growth[▽][†]

Jörg Toepel,[1] Eric Welsh,[2] Tina C. Summerfield,[1] Himadri B. Pakrasi,[2] and Louis A. Sherman[1]*

Purdue University, Department of Biological Sciences, 201 S. University Street, West Lafayette, Indiana 47907,[1] and Washington University, Department of Biology, Reebstock Hall, St. Louis, Missouri 63130[2]

We analyzed the metabolic rhythms and differential gene expression in the unicellular, diazotrophic cyanobacterium *Cyanothece* sp. strain ATCC 51142 under N_2-fixing conditions after a shift from normal 12-h light-12-h dark cycles to continuous light. We found that the mRNA levels of ~10% of the genes in the genome demonstrated circadian behavior during growth in free-running (continuous light) conditions. The genes for N_2 fixation displayed a strong circadian behavior, whereas photosynthesis and respiration genes were not as tightly regulated. One of our main objectives was to determine the strategies used by these cells to perform N_2 fixation under normal day-night conditions, as well as under the greater stress caused by continuous light. We determined that N_2 fixation cycled in continuous light but with a lower N_2 fixation activity. Glycogen degradation, respiration, and photosynthesis were also lower; nonetheless, O_2 evolution was about 50% of the normal peak. We also demonstrated that *nifH* (encoding the nitrogenase Fe protein), *nifB*, and *nifX* were strongly induced in continuous light; this is consistent with the role of these proteins during the assembly of the enzyme complex and suggested that the decreased N_2 fixation activity was due to protein-level regulation or inhibition. Many soluble electron carriers (e.g., ferredoxins), as well as redox carriers (e.g., thioredoxin and glutathione), were strongly induced during N_2 fixation in continuous light. We suggest that these carriers are required to enhance cyclic electron transport and phosphorylation for energy production and to maintain appropriate redox levels in the presence of elevated O_2, respectively.

Cyanobacteria have developed creative strategies that enable many strains to perform two incompatible processes, N_2 fixation and photosynthesis (10, 12, 13). Nitrogenase, the enzyme responsible for the fixation of atmospheric N_2 into ammonia, is rapidly and irreversibly inactivated upon exposure to molecular oxygen (10, 12). However, water is used as an electron donor for photosynthesis, which produces O_2 as a by-product. The strategies developed by diazotrophic cyanobacteria in order to perform both functions fall into two broad categories: spatial and temporal. The paradigm for spatial separation is based upon the heterocyst-forming, filamentous strains, such as *Anabaena* sp. strain PCC 7120 (17, 52). The heterocysts are specialized cells from which oxygen is excluded, due to the synthesis of a thick envelope that interferes with O_2 diffusion and in which photosystem II (PS II) is not produced. The nitrogen-fixing mechanism is activated in these cells in an environment very low in oxygen. Recent work has suggested that the cyanobacterial clade marked by such differentiation into heterocysts diverged once about 2,100 to 2,400 million years ago (48).

A variety of cyanobacteria utilize a form of temporal separation for the two processes. For example, nonheterocystous, filamentous cyanobacteria, such as *Oscillatoria* (44, 45), can develop alternate cycles for photosynthesis and N_2 fixation (3, 43). The marine, nonheterocystous, filamentous cyanobacterium *Trichodesmium* develops both temporal and spatial separation of N_2 fixation (5, 53). Although *Trichodesmium* does not form heterocysts, the nitrogenase localizes to a subset of cells within a trichome. In addition, nitrogenase shows a diurnal pattern in which its activity is highest early in the day (3, 6). Various results have shown that, under aerobic conditions, nitrogenase activity is modulated by the availability of reducing equivalents (33). This suggests that, in this organism, there is a competition for electrons between nitrogenase and respiration (43).

A number of different unicellular cyanobacteria exhibit temporal separation of photosynthesis and N_2 fixation when grown under light-dark (LD) cycles (14, 21, 22, 30, 36). We have utilized the unicellular, diazotrophic cyanobacterium *Cyanothece* sp. strain ATCC 51142 as a model organism for the study of such diurnal rhythms (7, 8, 34, 38–41). We have shown that nitrogenase transcription and translation are very tightly regulated when cells are grown in 12-h light-12-h dark cycles. The *nifHDK* operon is transcribed within the first few hours of the dark period, translated, activated, and then proteolytically degraded well before the end of the night (7). Photosynthesis also varies substantially throughout the daytime and reached a maximum at midday (4 to 6 h before the light period had ended), and photosynthetic capacity was at a minimum during the peak of nitrogenase activity in the early dark period (8, 41). Respiration reached a maximum at the same time as nitrogenase activity and quickly declined after the peak of N_2 fixation, thus providing some respiratory protection (32, 37). We demon-

---

* Corresponding author. Mailing address: Department of Biological Sciences, Hansen Hall, Purdue University, West Lafayette, IN 47907. Phone: (765) 494-8106. Fax: (765) 496-1496. E-mail: lsherman @purdue.edu.

† Supplemental material for this article may be found at http://jb .asm.org/.

▽ Published ahead of print on 4 April 2008.

strated similar rhythms with key metabolic storage products (25, 38, 40). For example, the fixed carbon from photosynthesis was stored in large glycogen granules that form between the photosynthetic membranes, and these granules subsume a large fraction of cellular volume by the end of the light period. The granules are quickly degraded in the dark as glucose is used as a substrate for respiration in order to generate energy and to utilize intracellular O_2 (40). The fixed nitrogen is stored in cyanophycin granules (composed of the amino acids Asp and Arg) that accumulate as the dark period progresses and then is utilized during the light period.

The above research was performed utilizing a small subset of the cellular genes and proteins. We analyzed the main nitrogenase genes, *nifHDK*, and major photosynthesis genes, such as *psbA*, *psbC*, *psbD*, and *psaAB*. The next stage in such studies required a sequenced genome, and *Cyanothece* sp. strain ATCC 51142 has now become one of some 30 cyanobacteria for which the entire genome has been sequenced (E. A. Welsh, M. Liberton, J. Stöckel, T. Loh, C. Wang, A. Wollam, R. S. Fulton, S. W. Clifton, J. M. Jacobs, L. A. Sherman, R. D. Smith, R. K. Wilson and H. B. Pakrasi, submitted for publication). *Cyanothece* has a rather interesting genome, with a 4.9-Mb circular chromosome, a 0.423-Mb linear chromosome, and four plasmids encoding a total of 5,269 predicted genes. The genome contains a contiguous set of 34 N_2 fixation genes that include *nifHDK* and genes encoding all of the proteins that are necessary to construct the metal clusters and the active nitrogenase. *Cyanothece* also has four complete copies of the *psbA* gene (plus a 75% fragment that is identical to *psbA1*) and three separate sets of genes encoding cytochrome oxidase.

Based on the first draft of this sequence, a microarray platform was developed (through Agilent) that included some 5,000 putative open reading frames (ORFs). The use of a 6-liter bioreactor enabled us to perform large-scale, temporal experiments on a single culture. We grew the cells in LD cycles and followed with a period of continuous light (LL) to determine the differences in transcription under these two conditions—one natural and one that places significant stress on the ability to fix N_2. This allowed us to identify those functions that were similarly regulated in LD and in LL and those functions that were altered in LL. We will discuss the results of the microarray experiments in relationship to a host of physiological parameters and outline the differences between LD and LL growth under N_2-fixing conditions.

MATERIALS AND METHODS

Bacterial strains and growth conditions. *Cyanothece* sp. strain ATCC 51142 cultures were grown in an airlift bioreactor (6-liter BioFlo 3000; New Brunswick Scientific, Edison, NJ) in ASP2 medium without nitrate at 30°C in 12-h light-12-h dark cycles (38). The design of the bioreactor was modified to optimize cyanobacterial growth and to continuously measure parameters such as pH value, temperature, and dissolved oxygen (Mettler-Toledo Instruments, Urdorf, Switzerland). To provide even illumination in the culture, a glass cylinder with a small diameter of 13 cm (height, 50 cm) and dilute cell cultures (optical density at 750 nm, <0.2) were used. The culture was illuminated by two light-emitting-diode panels using alternating arrays of orange (640 nm) and red (680 nm) light-emitting diodes, yielding an intensity of ~100 μmol photons m^{-2} s^{-1} inside the bioreactor (underwater quantum light meter LI 192; Li-Cor, Lincoln, Nebraska). Cultures were inoculated into the bioreactor at a cell density of approximately 1×10^6 cells ml^{-1} and were grown for 5 to 6 days under LD conditions prior to taking samples.

This bioreactor permitted us to monitor a number of physiological parameters during growth, particularly pH and dissolved oxygen. We also took samples for 18 h per day (hour 0 of the light period [L0] to hour 6 of the dark period [D6]) for measurement of cell number, chlorophyll *a* (Chl *a*) concentration, photosynthetic O_2 evolution and respiration, and glycogen content (50 ml per time point), since the results of many previous experiments indicate that D6 was the peak for N_2 fixation. The cell number and Chl *a* concentration were measured by using a Petroff-Hauser cell count chamber and a Perkin-Elmer spectrophotometer (Lambda 40; Shelton, CA), respectively, as described previously (38). Photosynthetic oxygen evolution (using a growth light intensity of 100 μmol photons m^{-2} s^{-1} for illumination) and respiration rates (monitored as O_2 consumption in the dark) were determined using a Clark-type electrode (Hansatech, Norfolk, England) without adding bicarbonate. N_2 fixation rates were determined by measuring ethylene on a Hewlett Packard 8460 gas chromatograph (Wilmington, DE) and calculated as described previously (7). Briefly, 2-ml samples were incubated with 2 ml acetylene in 10-ml incubation tubes for 1 h in the light or in the dark according to the point of time in the LD cycle. The rates of photosynthesis, respiration, and N_2 fixation shown in Fig. 1 are plotted on the right axis as relative activity. Photosynthesis is represented as O_2 evolution (positive activity), whereas respiration is represented as O_2 uptake (negative activity). This experimental protocol was repeated six times with essentially identical results.

Microarray platform. The microarray platform consisted of 5,048 ORFs based upon the rough draft of the *Cyanothece* genome sequence that was obtained by the Washington University Genome Center. The ORFs were identified by using Critica and Glimmer (Welsh et al., submitted). The 60-mers appropriate for each gene were determined by using a computer program written by Rajeev Aurora, St. Louis University, St. Louis, MO, and provided by him to Agilent, Inc. (Santa Clara, CA). The microarrays were fabricated with each probe printed in duplicate by Agilent, and these arrays, along with the purified RNA samples, were given to MoGene (St. Louis, MO) for hybridization, scanning, and initial data analysis.

RNA isolation. For the microarray experiment, 300-ml samples were taken every 4 h over a 48-h period that included a complete LD cycle and 24 h of LL. The cells were centrifuged at 5,000 × *g* and resuspended in STET-buffer (8% sucrose, 5% Triton X-100, 50 mM EDTA, 50 mM Tris-HCl, pH 8, with diethyl pyrocarbonate water) and stored at −80°C. The RNA extraction was performed with Tri-Reagent (Ambion, Austin, TX) according to the manufacturer's protocol. Briefly, the samples were incubated for 5 min with Tri-Reagent and washed with glass beads (1 min of vortexing) at room temperature and 1-bromo-3-chloropropane was used for phase separation. RNA was precipitated with isopropanol, and RNA clean-up kit-5 columns from Zymo Research Corporation (Orange, CA) were used to remove contamination (e.g., carbohydrates and organic solvents).

The hybridization control consisted of a mixed sample that contained equal amounts of RNA from each time point. The results are for a combination of four biological and two technical replicas. For each microarray, 7 μg RNA was used (3.5 μg sample plus 3.5 μg control). Total RNA was labeled with either cyanine-5 or cyanine-3 by using a ULS RNA fluorescent-labeling kit from Kreatech Biotechnology (Amsterdam, The Netherlands) according to the manufacturer's protocol. The labeled material was passed through Zymo RNA clean-up kit-5 columns (Zymo Research Corporation, Orange, CA) to remove unincorporated label and eluted in 15 to 20 μl of RNase-free water. The concentration of labeled total RNA and label incorporation was determined on a Nanodrop-1000 spectrophotometer (Wilmington, DE). All of the labeling and postlabeling procedures were conducted in an ozone-free enclosure to ensure the integrity of the label. Labeled material was hybridized for 17 h in a rotating oven at 65°C in an ozone-free room. The wash conditions used were as outlined in the Agilent processing manual (Santa Clara, CA), and the arrays were scanned using an Agilent scanner. Analysis was performed by using Agilent's Feature Extraction software version 9.1 and Rosetta Luminator software.

Semiquantitative RT-PCR. RNA was treated with DNase I (Invitrogen, Carlsbad, CA) for 1 h at 37°C and successful DNase I treatment was confirmed by PCR for each RNA sample. Reverse transcription (RT) was performed by using Superscript II (Invitrogen, Carlsbad, CA) and random primers following the manufacturer's instructions. PCR was carried out with 94°C for 1 min, 30 cycles of 94°C for 30 s and 54°C for 30 s, and 68°C for 30 s to amplify regions of the genes *nifD*, *coxC1*, and *rpnA*. Due to the high transcript level of these genes, amplification using *psbA* and *psbD* primers was performed using 20 cycles of the PCR conditions described above. The *rpnA* transcript abundance was used as a control, since microarray data indicated that the transcript level for this gene was unchanged under these growth conditions. The primers and amplified-product sizes for each transcript were as follows: *nifD*, F GGTGGAGACAAAAAAC TCGC and R TACCACACGAAGACCGATT (384 bp); *psbA1*, F CTTAATCT
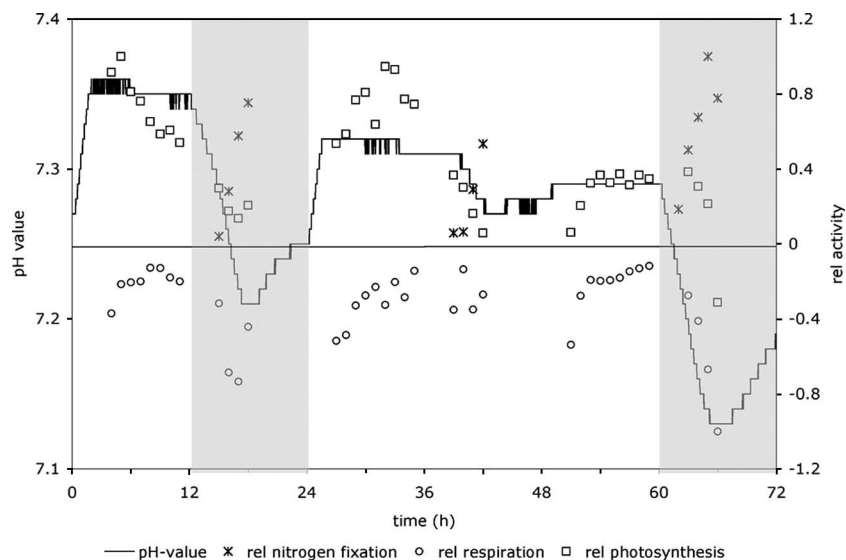
FIG. 1. Plot of the physiological parameters of *Cyanothece* sp. strain ATCC 51142 during growth in a 6-liter bioreactor during 12-h light–12-h dark periods followed by 36 h of light and a final 12-h dark period. Grey areas represent dark periods. The parameters monitored were pH (left ordinate); nitrogenase activity (acetylene reduction); and respiration and photosynthesis, measured as O_2 uptake and O_2 evolution, respectively. Photosynthesis is represented as O_2 evolution (positive activity), whereas respiration is represented as O_2 uptake (negative activity). The relative rates of the later three parameters are shown (right ordinate), and the maximum values were nitrogenase, 196 nmol N_2 10^8 cells^{-1} h^{-1}; respiration, 275 μmol O_2 mg Chl a^{-1} h^{-1}; and photosynthesis, 250 μmol O_2 mg Chl a^{-1} h^{-1}. rel, relative.

ACCCCATCGGAC and R AGGCCATGCACCTAAGAAGA (363 bp); *coxC1*, F CATGCACAAAGGACAAACCG and R GCCGAAAAAGGACTCACTTG (276 bp); *rnpA*, F GGATTACCCAAACAACACCG and R CTTGACCACAA TCACCACCT (275 bp); and *psbD*, F AGGTGTTCTCGGTGGTGCTTTACT and R ACCGACAATACCGATCGCACTCAT (290 bp).

FTIR spectroscopy. The macromolecular composition of the cells was determined over the 48-h period with a Fourier transform infrared (FTIR) spectrometer (Thermo-Electron, Madison, WI). Samples (2 ml) were taken every 4 h over a 48-h time period (one complete LD cycle and 24 h LL), washed twice with distilled water, and stored at −80°C. The cells were dried prior to measurement on an IR slide at 45°C for 4 h. For each sample, 128 spectra × 50 spots were measured and analyzed according to the method of B. Penning (see http://cellwall.genomics.purdue.edu/). The spectra for each sample were baseline corrected, area normalized, and averaged.

Microarray data accession number. The entire microarray data set, entitled "*Cyanothece* sp. ATCC 51142 12 h light + 12 h dark + 24 h light in a 48 h time course," has been deposited into ArrayExpress (http://www.ebi.ac.uk/aerep/) under accession no. E-TABM-386.

RESULTS

Physiology: photosynthesis, respiration, and N₂ fixation. Figure 1 shows the results for photosynthetic activity (the values in the gray areas represent the potential activity), respiration, and N_2 fixation during the experiment. Since each light or dark period was 12 h long, we designated each phase as D0 to D12 or L0 to L12 (L0 = D12 and D0 = L12). The pH value and the O_2 concentration increased at the beginning of the light period; the pH stayed constant throughout the light period, whereas the O_2 concentration declined in the second half of the light period, after L6. The photosynthetic O_2 evolution, measured on a Clark electrode, reached a maximum at L6 and declined after this time point. During the dark phase, the pH value decreased, as did the level of dissolved O_2 (data not shown); respiration rates were high; and the potential photosynthetic rates were low. The peak of N_2 fixation occurred at D6 during the normal LD cycle (Fig. 1). This time point also

represented the peak of respiration activity and the concomitant decrease in pH; the pH increased and respiration rates decreased during the remainder of the dark period.

We then applied a 36-h LL regime to the culture, so that the period between 36 h and 48 h in Fig. 1 represents a subjective dark phase. The light period from 24 h to 36 h proceeded in a fashion similar to that in the previous light period. However, as cells proceeded into the subjective dark phase, the pH initially decreased but only changed by about one-third of the amount observed in the normal dark period (LD cycle). The respiration rates during this time period were only 50% of the rates in the dark. However, the decline in photosynthetic rates in the subjective dark period was almost identical to the real dark-period rates. The nitrogenase activity reached a maximum at the same time point as in the normal LD cycle (after 42 h [D6]) but at only half the LD cycle rate. As the culture proceeded into the subjective light period, the pH changed very little and the photosynthetic oxygen evolution was less than 40% of that seen in the LD cycle. Once cells were returned to the dark, there was a steep decrease in pH, a sharp increase in respiration, and a significant nitrogenase activity peak at D5 that was more than 25% higher than the normal LD cycle rate.

Gene expression. As described in Materials and Methods, 12 RNA samples were collected at 4-h intervals during one LD cycle and 24 h of LL. Including dye swaps, a total of 24 arrays on 12 slides were used for the hybridizations. The statistical analysis indicated that the results were highly significant and that meaningful comparisons could be made among all of the data. A conservative twofold variation in the differential expression levels during these cycles permitted us to identify 1,424 genes (approximately 20% of the entire genome). We demonstrated previously that *Cyanothece* cells showed a strong circadian behavior (41), and we anticipated that the genes of
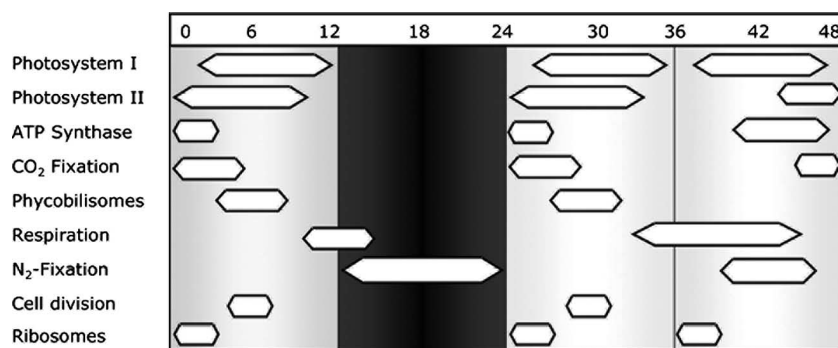
FIG. 2. Diagram of differential gene expression of *Cyanothece* sp. strain ATCC 51142 grown in 12-h light and 12-h dark periods followed by 24 h of LL; the times are the same as in Fig. 1. Dark grey represents the dark period. Data for the key functional categories of photosynthesis, respiration, N₂ fixation, cell division, and ribosomal proteins are depicted. The bars represent the time periods when many genes within a category are up-regulated twofold or more.

the measured processes would show similar regulation in the dark and the subjective dark periods.

We analyzed the LD-dependent (diurnal) and dark-independent (circadian) gene expression of the genes whose transcript levels were up-regulated twofold or more during the 48-h experiment. About 750 of those genes were up-regulated during the light periods, including the genes for the photosynthesis apparatus, ATP synthase, and glycogen synthesis (see overview in Fig. 2). In addition, ~650 genes were up-regulated during the true dark period, including genes for N₂ fixation, respiration, and glycogen degradation. The gene expression pattern in the second light period was almost identical, with 80% of the same genes up-regulated. However, differences occurred during the subjective dark period, resulting in a reduction of the number of up-regulated genes (down to 60% of the number in the true dark period) and a quantitative damping effect of the gene expression levels relative to the levels in the true dark period. Additionally, ~200 genes showed further up-regulation during this period (see below).

Genes exhibiting circadian behavior included genes that were up-regulated during the subjective dark period (twofold or greater increase) in comparison to their expression during the real light period and had an expression pattern identical to that in the real dark period. Additionally, we defined as circadian those light-up-regulated genes with a twofold or greater down-regulation in transcript level during the subjective dark period. This group of genes with changes in transcript levels consistent with circadian regulation consisted of around 10% of the total genome.

Figure 2 provides an overview of the gene expression pattern during the 48-h period, including both the LD and the LL cycle. Thus, N₂ fixation genes were up-regulated in the dark and during the subjective dark but with some differences that will be discussed later. Ribosomal genes that normally were up-regulated during the early light period were also up-regulated during the beginning of the subjective dark period. Genes involving various components of the photosynthetic apparatus were typically up-regulated in the light and toward the end of the subjective dark period; this is in good accordance with what was shown before with a subset of such genes (41). We determined that the tight synchrony for PS II, ATP synthase, and CO₂ fixation genes was lost under LL conditions. PS I and ATP

synthase genes were altered to an even greater extent, and transcription of the main PS I genes remained high throughout the LL period. Most interestingly, genes encoding the respiratory proteins were transcribed late in the light period and into the early dark period (Fig. 2), and a similar pattern was seen during growth under LL conditions.

The full impact of such temporal regulation of gene expression throughout the LD and LL cycles is shown in Fig. S1 in the supplemental material (accompanied by the complete data set in Fig. S2 [available at http://www.biology.purdue.edu/sherman/]). This type of network, constructed using Cytoscape, clusters genes based on their temporal transcription patterns and permits spatial analysis of various functional categories. From such patterns, we can see that specific categories of genes, such as certain N₂ fixation genes, photosynthesis genes, and ribosomal genes, were light responsive. We will discuss some of the more-important transcriptional changes in the following sections.

The comparison of differential gene transcription between the dark period and the subjective dark period yielded four groups of genes: (i) genes that were not affected by the incident light and genes that had a reduced expression level in the subjective dark relative to their expression in the dark period (these genes were up-regulated in comparison to their expression in the light period, but not as much as in the real dark period) (Fig. 3A); (ii) genes that were up-regulated in the light and low in the dark but up-regulated in the subjective dark (Fig. 3B); (iii) genes that were up-regulated during the subjective dark period, but not in the dark (Fig. 3C); and (iv) genes which were up-regulated during the dark, but not in the subjective dark (Fig. 3D). We focused our analysis on the third and fourth categories of genes, since these genes showed a direct response to the changing light conditions. We found several genes that were up-regulated only in the real dark period; e.g., several two-component hybrid sensors/regulators, the uptake hydrogenase (both *hupL* and *hupS*), one copy of the *psbA* gene, and several genes encoding unknown proteins (Fig. 3D). The CheY-like response regulator whose expression is shown in Fig. 3D (cce_1982) is located very close to the cytochrome oxidase operon (cce_1975 to cce_1977), and these genes demonstrated virtually identical kinetics—transcription increased strongly around L10 and reached a peak at D2. This regulator is similar to the response regulator slr0474 in *Syn-*
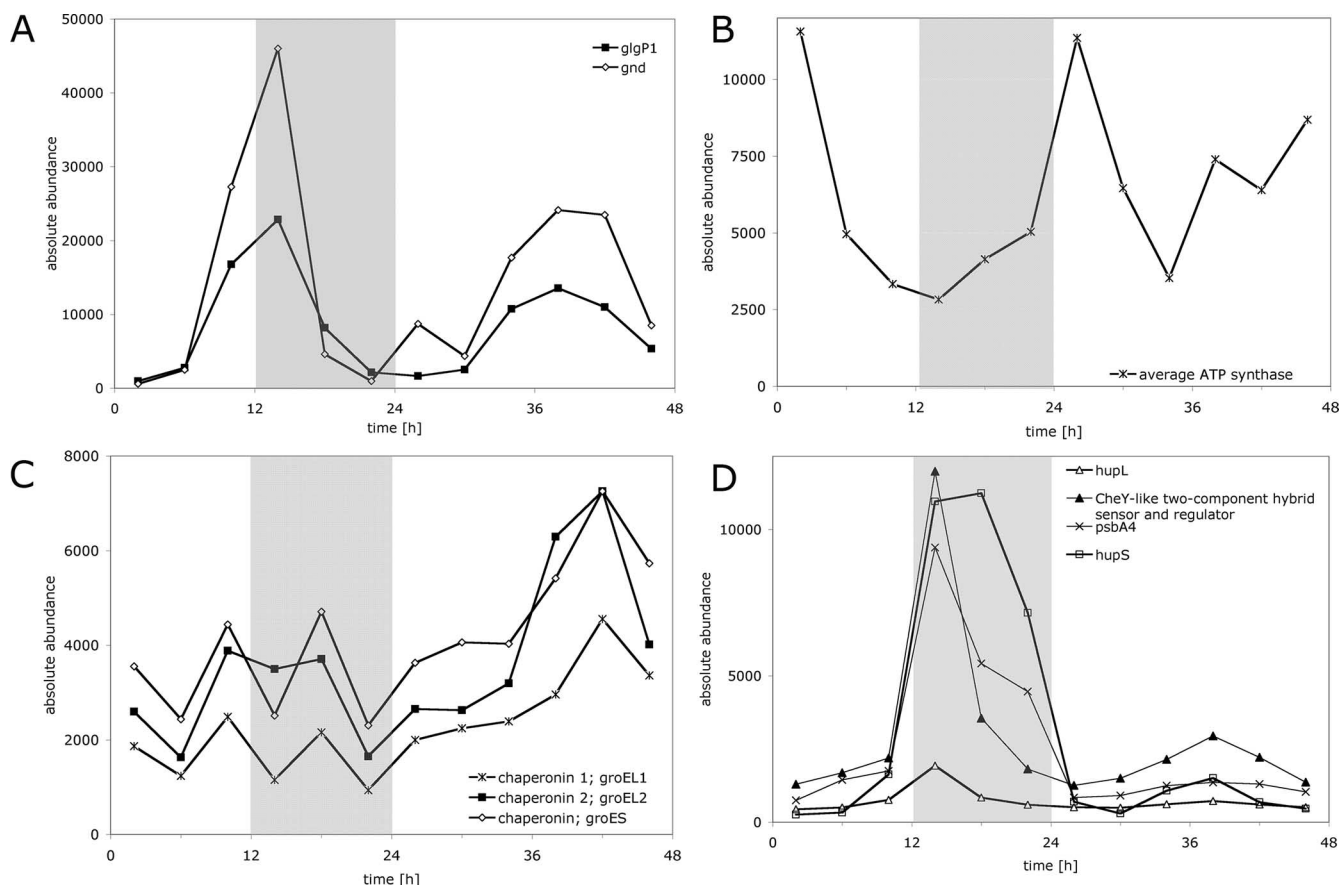
FIG. 3. Transcriptional kinetics of specific genes during diazotrophic growth in LD and LL in the cyanobacterium *Cyanothece* sp. strain ATCC 51142. Grey represents the dark period. (A) Class of genes whose expression increased in the subjective dark but less than in the dark: *gnd* and *glpP1*. (B) Genes that were up-regulated in the light and also in the subjective dark: ATP synthase genes. (C) Class of genes whose expression was increased more in the subjective dark than in the dark: *groELS* and *groEL2*. (D) Class of genes that were greatly induced in the dark and much less so in the subjective dark: *hupLS*, *psbA4*, and a gene encoding a CheY-like response regulator (cce_1982) that was near the dark-inducible *cox* operon.

echocystis sp. strain PCC 6803 and is contiguous to a gene (cce_1983), slr0473, encoding a phytochrome-like protein (77% similarity) in *Synechocystis* sp. strain PCC 6803. Of the ~100 histidine kinases in the *Cyanothece* genome, around a dozen displayed regulatory patterns that indicated a possible involvement in LD control under N_2-fixing conditions (data not shown). Several response regulators that contained PAS groups and other domains that may indicate an involvement with LD regulation are located near histidine kinases. Another group of genes that showed an increase in gene expression included two genes with a 4VR motif (cce_1209 and cce_1212). These genes were on either side of genes encoding a globin gene and a ferredoxin gene, and all four demonstrated similar increases in gene expression. These genes were normally up-regulated during the beginning of the light period and showed up-regulation at the beginning of the subjective dark period. The functional importance of the proteins encoded by this gene cluster is unknown, but comparison to results for *Synechocystis* sp. strain PCC 6803 (42) suggested that they may be involved in redox regulation. Furthermore, we found evidence that the potential LD response regulator (*cph1*) in *Synechocystis* sp. strain PCC 6803 (15) is also responsible for the dark

reception in *Cyanothece*, and it is up-regulated at the beginning of the normal dark periods, but not in the subjective dark period.

The analysis of genes with circadian behavior that were specifically up-regulated in the subjective dark period compared to normal LD growth yielded some 200 genes, and a selected group is highlighted by functional category in Table 1. Interestingly, the genes for stabilizing PS II O_2 evolution (e.g., *psbO* and *psbQ*) and many PS I genes were up-regulated during the subjective dark. A major change occurred in the expression levels of numerous ferredoxin-related proteins and ferredoxin reductases. Additionally, *petH* was up-regulated during the subjective dark period and, if one includes the cytochrome genes (e.g., the cytochrome b_6f genes), all genes for cyclic electron flow were up-regulated at least twofold during the subjective dark. In addition, several genes encoding proteins involved in maintaining the redox balance were up-regulated in the subjective dark.

One of the particularly intriguing differences between growth in LD and LL was found among the genes encoding nitrogenase proteins (Fig. 4). The transcript levels for *nifH* were always three- to fourfold higher than those of *nifDK* (as

TABLE 1. Change in transcript level of selected genes between subjective dark (36 to 48 h of LL) and dark (D12 to D24)

Gene(s); function	Fold change[a]
Stress response genes	
clpP3, -4, clpC; Clp protease-encoding genes	2–3
groES, groEL	2–3
Bacterial stress gene	2–3
Other protease-encoding genes	2–3
Photosynthesis genes	
PS II, PS I genes	
psbO	2
psbQ	1.6
psaB, -D, -E	2–3
petH; Fd-NADP-oxidoreductase	3
ATP synthase genes	
atpAEGH	2
Cytochrome b_6f complex genes	
petC1, -D, -B, -N	2–3
N_2 fixation genes	
nifB; regulation	5[b]
nifW; folding/protection	3[b]
nifX; folding	3[b]
Soluble electron carrier and redox component genes	
petE, plastocyanin	2
petF1, -3, -4; ferredoxin	4
fdxB; ferredoxin	3
ftrC; Fd-thioredoxin-reductase	3
trxM2, -A1; thioredoxin	1.5–3
gst1, glutathione-*S*-transferase	3
glnA, glutamine synthetase	3–4
Respiration and glycolysis genes	
ndhDFHIFM; NADH dehydrogenase	2
coxA1, -B1, -C1	2
gap1; glyceraldehyde dehydrogenase	2
Fatty acid genes	
desC, -A	2
Glycogen synthesis and breakdown genes	
glgX; debranching	0.8
glgP; phosphorylase	1.5
glmM, glgA, -B, glpX	2
Pentose phosphate pathway genes	
gnd; 6-phosphogluconate-dehydrogenase	4
zwf; glucose-6-PO_4-dehydrogenase	2
tktA; transketolase	2

[a] Increase in expression during hours 36 to 48 of LL from levels during D12 to D24.
[b] Up-regulated at 42 h LL only in comparison to the level at D18.

well as higher than those of all of the other genes encoding Nif proteins) throughout the dark as well as the LL periods. The *nifH* transcript level was particularly high in LL, and the peak in both cycles was at D6. Unexpectedly, the *nifB* and *nifX* genes also showed substantial changes between the dark and the subjective dark periods. In the dark, *nifB* and *nifX* transcription peaked at D2 and then declined throughout the remainder of the dark. On the other hand, in the subjective dark, *nifB* and *nifX* reached much higher peaks at D6 (the same

time at which *nifH* reached a maximum) and then declined sharply (Fig. 4).

Glycogen composition. We hypothesized that one reason for the smaller nitrogenase peak in LL and the small change in pH was a lack of carbohydrate supply; e.g., the low degradation rates of glycogen granules in LL compared to LD conditions. We therefore determined the glycogen content using an FTIR spectrometer, which permitted careful analysis with small culture volumes. The absorption maxima of the IR spectra can be assigned to different macromolecules (24). The absorption around 1,000 to 1,200 cm^{-1} can be assigned to carbohydrates, and an increased absorption at these wave numbers is a result of an accumulation of carbohydrates. We analyzed the carbohydrate content every 4 h and compared the difference spectrum for L10 minus D10 with a spectrum taken from pure glycogen (see Fig. 5). It can be seen that the increase of the absorption in the specified wave number region is a result of carbohydrate accumulation during the light period. Therefore, we used integrated area values for the measure of the relative carbohydrate content, and since the main storage product is glycogen, as glycogen content. Figure 5 (inset) shows the variation of the absorbance in the specified area. The relative glycogen accumulation reached a maximum at D2 for the LD-grown cells, in agreement with data obtained using biochemical techniques for cultures grown in 250-ml Erlenmeyer shake flasks (38). As expected, the glycogen content decreased in the dark and increased again during the subsequent light period (24 h to 36 h). However, glycogen content did not decline in the subjective dark period (36 h to 48 h) and continued on to an even higher plateau than at 12 h (Fig. 5, inset). Thus, glycogen was not utilized to the same extent in LL as in the LD cycle, and this was consistent with our hypothesis. We were able to verify these results by utilizing high-pressure freeze cryoelectron microscopy (data not shown). Therefore, we concluded that the net production of glycogen was higher than the
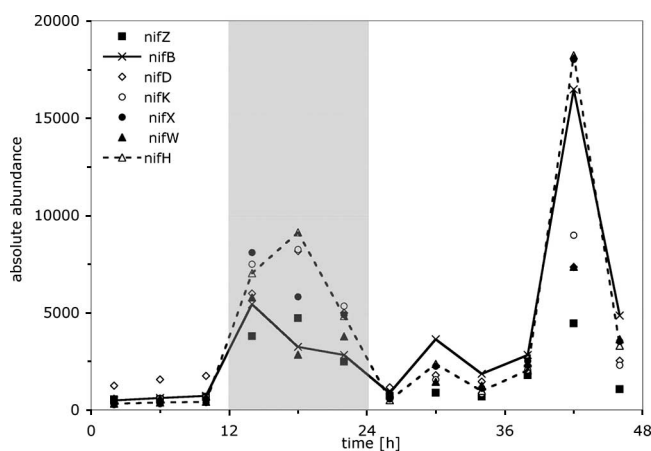
FIG. 4. Transcriptional kinetics of some key nitrogenase genes during diazotrophic growth in LD and LL in the cyanobacterium *Cyanothece* sp. strain ATCC 51142. Grey represents the dark period. Results for the genes encoding NifH and NifDK, along with some of the genes important in the assembly of the FeMo cofactor, are displayed. The levels of NifH were fourfold higher than the levels on the left ordinate, but the curve was compressed to better highlight the transcriptional kinetics of the other genes.

FIG. 5. Determination of glycogen content as measured by FTIR spectroscopy. The difference spectrum between cells from D10 (containing no granules) and L10 (filled with granules) is compared to a pure glycogen reference. The qualitative comparison between these curves indicated that the measurements of the integrated 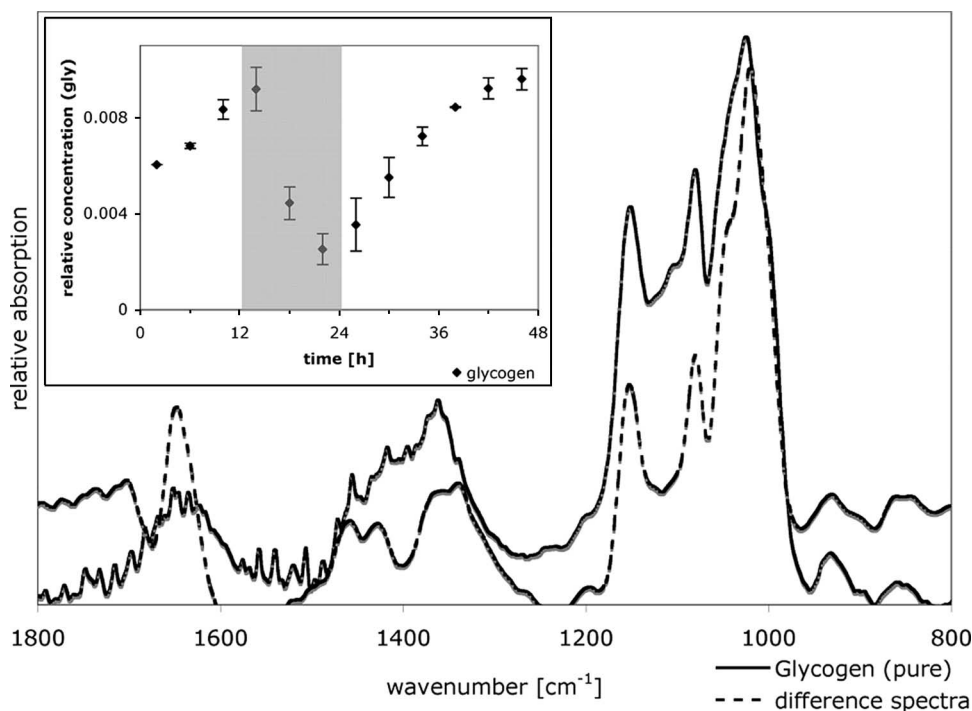area at wave numbers between 1,200 and 1,000 cm^{-1} were a good monitor of intracellular glycogen. The inset demonstrates these measurements every 4 h through an LD cycle followed by a 36-h period of LL. Grey represents the dark period. Error bars show standard deviations. gly, glycogen.

breakdown from glycogen granules or that the breakdown was somewhat inhibited under LL conditions.

Our microarray experiment results led to the conclusion that the high level of glycogen during the subjective dark was not a result of a differential gene expression. The glycogen phosphorylase (*glgP1*) and the glycogen-debranching enzyme (*glgX*) showed nearly the same expression levels in the subjective dark as in the dark (Fig. 3A). In contrast, the glycogen synthetase (*glgA1*) had the same expression level as in the light but was twofold up-regulated in comparison to its level in the true dark period. These results suggest that either the net production of glycogen is higher than the breakdown in the subjective dark or that posttranscriptional regulation prevented glycogen breakdown.

The lack of energy for N$_2$ fixation, normally supplied by glycogen, can be provided through the tricarboxylic acid cycle and the pentose phosphate pathway since most of these genes were transcribed throughout the LL period (data not shown). A particularly notable example was *gnd*. Under LD conditions, its transcript level was high in the early dark and then declined sharply throughout the dark period, but the transcription levels had a lower and broader peak during LL growth (Fig. 3A).

Validation. We used RT-PCR to validate the results of the microarray experiments. Figure 6 shows a comparison between the microarray results and the RT-PCR results for a select set of genes that demonstrated different types of temporal expression. This included *nifD* that was expressed only in the dark/subjective dark and two PS II genes (*psbA1* and *psbD*) that were transcribed primarily in the light. We also compared the
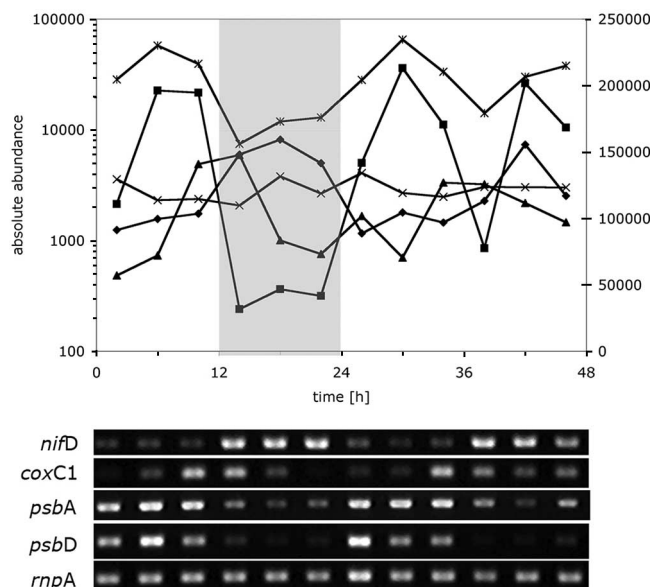
FIG. 6. Validation of the microarray results by comparison with the results from RT-PCR experiments. The genes chosen are examples of different categories of differential expression and include *nifD* (◆), highly expressed in the dark; *coxC1* (▲), highly expressed at the end of the light period and into the dark period; *psbA* (■) and *psbD* (∗), highly expressed in the light; and *rnpA* (×), little change in expression throughout the experiment. Grey represents the dark period.

results for *coxC1*, which was transcribed at high levels toward the end of the light period and into the early dark period (L10 to D2). It can be seen that there is a very close correspondence between the microarray data and the RT-PCR data for all three types of regulation. These should be compared to the results for *rnpA*, which were virtually unchanged in both the microarray and the RT-PCR experiments. Based on these results, we concluded that the microarray results were a fair representation of differential gene expression in this organism under these LD and LL conditions.

DISCUSSION

Our experimental setup allowed a genome-wide determination and differentiation of diurnal and circadian (LD independent) controlled genes in a unicellular diazotrophic cyanobacterium. This study provides a genome-wide overview of LD-independent transcript levels, and subsequent promoter analysis of the genome can delineate the complete circadian regulation. We determined that 20% of the total genome displayed a diurnal expression pattern (in good accordance with the results of Stöckel et al. [46]). However, 60% of the genes associated with the dark period, including genes for N_2 fixation and respiration, were regulated independently of the incident light and were also up-regulated in the subjective dark period.

We demonstrated that N_2 fixation occurred during LL as shown previously (7), albeit at a reduced level. This reduced level appeared to be due to a confluence of factors. The rates of photosynthesis were lower during the subjective dark period than during the previous light period, but O_2 evolution was still a significant process. Respiration became prominent by 2 h into the subjective dark but never reached the level seen in true darkness. The rates of O_2 consumption continued at a low level throughout the remainder of LL growth. We also determined that the glycogen granules were more prevalent and larger during LL and that the level of glycogen remained higher under LL conditions. It is likely that the oxygen levels could be higher under conditions where O_2 evolution iss greater than O_2 uptake, and this can affect nitrogenase activity. These results suggest strongly that the level of N_2 fixation is dependent upon respiration, either for energy production or for removal of intracellular O_2. This hypothesis is supported by the results for the subsequent dark period, in which glycogen breakdown and respiration were extremely high, as was the resultant peak of N_2 fixation (Fig. 1).

One important response in the subjective dark was the up-regulation of *psbA4*, one of the genes encoding the D1 reaction center protein. This gene is transcribed at very low rates under light conditions, but its transcript level increased dramatically in the dark, coincident with the peak of nitrogenase activity. This protein has an amino acid sequence that is significantly different from that of *psbA1*; in particular, it has many changes in the amino acids near the C terminus that are involved with binding Mn and, thus, with the evolution of O_2. We hypothesize that the incorporation of *psbA4* into PS II leads to PS II complexes that are incapable of O_2 evolution. This would limit the amount of intracellular oxygen in the dark but still provide PS II centers that can then be reconstituted with copies of more-active D1. On the other hand, this response is not seen in LL, suggesting that this is one reason why it is more difficult to

provide an appropriate environment for an active nitrogenase. Overall, we conclude that the decrease in the photosynthetic oxygen evolution is a result of several processes, including cyclic electron flow with electrons provided by an alternative electron donor and state transitions (37), as well as non-O_2-evolving complexes.

The transcript level of the global nitrogen regulator *ntcA* (cce_0461) was low during the entire experiment, in agreement with the results of Bradley and Reddy (4). Therefore, we conclude that *ntcA* is not involved in the regulation of N_2 fixation under our conditions. However, the up-regulation of *ntcB* during the dark period indicated a function in nitrogen assimilation or an activation of nitrate assimilation (1, 2) even under nitrate-limiting conditions. Another nitrogen-related gene, a glutamine synthetase inhibitor (IF7, cce_0259) was up-regulated in the light and down-regulated during the dark and the subjective dark periods. Glutamine synthetase was up-regulated at the end of the light and beginning of the dark period and during the subjective dark period. Therefore, the reduced N_2 fixation rates in the subjective dark period are not a result of lack of transcript of this enzyme.

One main objective of this work was to determine the differences between periods of N_2 fixation in the dark versus the subjective dark. In particular, can we identify the specific strategies that the cell uses to ensure the proper functioning of nitrogenase under the more-hostile conditions found in LL? It is clear from the results depicted in Fig. 4 that the decrease in the levels of nitrogenase activity was not caused by decreased transcription of the *nifHDK* genes. In the subjective dark, the transcript levels of *nifDK* were very similar to those seen in the dark, whereas the transcript levels for *nifH* were some twofold higher in the subjective dark. These results are similar to what has been shown for other cyanobacteria in that higher O_2 levels affect nitrogenase activity and not *nifHDK* transcription (6, 50). The high level of transcription of *nifH* versus *nifDK* is similar to the situation in *Azotobacter vinelandii*, where *nifH* transcript levels are approximately fourfold higher than those of *nifDK* (23). This is consistent with the functional role of the Fe protein (NifH) with respect to the MoFe protein (NifDK) (35, 47). Importantly, because *nifH* transcript levels doubled between D6 (real dark) and D6 (subjective dark), the ratio of *nifH* transcripts to that of *nifDK* increased to almost 10:1 in the subjective dark. Thus, one transcriptional strategy for N_2 fixation during LL growth is to help ensure sufficient Fe protein for efficient function and, possibly, to ensure proper assembly of the full NifDK complex.

Interestingly, the transcript levels for *nifB* and *nifX* were also significantly higher in the subjective dark and qualitatively and quantitatively similar to the transcript level of *nifH*. This pattern would be consistent with the recent model for the synthesis of the FeMo cofactor prior to its insertion into the apodinitrogenase (NifDK) to generate the mature dinitrogenase (9, 18, 19, 20, 27). This suggests that high turnover rates of nitrogenase provide active enzyme complexes for N_2 fixation despite the presence of higher intracellular O_2 levels. It is notable that FeS proteins play an important role in *Azotobacter vinelandii*, possibly by forming a complex with nitrogenase to generate an inactive but oxygen-stable enzyme complex (28, 29, 49) This process is termed conformational protection, but we could not identify a similar protein in *Cyanothece*; however, we

found that many ferredoxins and many soluble electron carriers showed enhanced transcript levels, possibly implying an involvement in oxygen scavenging. These electron carriers can enhance additional routes for electron transport (e.g., to enhance cyclic electron transport, N_2 fixation, and phosphorylation). We suggest that redox carriers, such as thioredoxin and glutathione, are synthesized in the subjective dark period to maintain appropriate redox levels in the presence of elevated O_2 and subsequent oxidative-stress conditions. Although it would seem possible that oxidative-stress-response genes, such as catalase or superoxide dismutase, would be induced in LL (51), none of the genes annotated with these functions were up-regulated in the subjective dark period. Finally, the genes of the pentose phosphate pathway enzymes demonstrated higher transcript levels, possibly in order to enhance reducing power in the cell as photosynthesis declined.

What then leads to the lower levels of nitrogenase activity in LL growth? When we factor in the inability to break down the glycogen granules and the resulting decrease in respiration, these results suggest that the reduction in nitrogenase activity was due to a decline in respiration, leading to lowered energy levels and to an enhancement of intracellular O_2 levels. Thus, concurrent photosynthetic energy production was required, leading to additional O_2 evolution. Peschek et al. (32) demonstrated that the lack of carbon skeletons limits the nitrogenase activity. Additionally, Oelze (31) demonstrated that it was not oxygen levels that reduced the nitrogenase activity but the reduction in levels of ATP supplied via respiration. The most-striking finding was that the levels of glycogen, stored in increasingly dense glycogen granules, remained high in the subjective dark. This can be a result of the thioredoxin regulation (activation) of glycogen synthesis, demonstrated by Lindahl and Florencio (26) in *Synechocystis* sp. strain PCC 6803. This result, plus the up-regulation of ferredoxins and thioredoxins in the subjective dark period, is consistent with our hypothesis that glycogen accumulation is a result of light-induced net production (11, 26). Furthermore, Gómez Casati et al. (16) demonstrated that glycogen synthetase is sensitive to several regulators and metabolites and is activated by 3-phosphoglyceric acid, which can be produced during the light and subjective dark period. We suggest that the higher expression of genes encoding proteins involved in cyclic electron flow of the photosynthetic apparatus leads to higher ATP production and thus reduced the level of noncyclic electron flow and concomitant oxygen evolution in the subjective dark period. This is supported by previous measurements of state transitions that indicated a connection of the phycobilisomes with PS I during the dark period (41). The "energy shortage" was released upon placing the cells in the dark, and this led to very large rates of respiration and N_2 fixation.

These transcriptional results provide an important framework with many specific hypotheses that can be tested further. One next step in our studies will be a thorough proteomics analysis of proteins synthesized during an LD and an LL growth experiment. We will concentrate specifically on the subsets of proteins mentioned above and determine the relationship of transcriptional and translational regulation in this intriguing process.

REFERENCES

1. **Aichi, M., and T. Omata.** 1997. Involvement of NtcB, a LysR family transcription factor, in nitrite activation of the nitrate assimilation operon in the cyanobacterium *Synechococcus* sp. strain PCC 7942. J. Bacteriol. **179:**4671–4675.
2. **Aichi, M., N. Takatani, and T. Omata.** 2001. Role of NtcB in activation of nitrate assimilation genes in the cyanobacterium *Synechocystis* sp. strain PCC 6803. J. Bacteriol. **183:**5840–5847.
3. **Berman-Frank, I., P. Lundgren, Y. B. Chen, H. Kupper, Z. Kolber, B. Bergman, and P. Falkowski.** 2001. Segregation of nitrogen fixation and oxygenic photosynthesis in the marine cyanobacterium *Trichodesmium*. Science **294:**1534–1537.
4. **Bradley, R. L., and K. J. Reddy.** 1997. Cloning, sequencing, and regulation of the global nitrogen regulator gene *ntcA* in the unicellular diazotrophic cyanobacterium *Cyanothece* sp. strain BH68K. J. Bacteriol. **179:**4407–4410.
5. **Chen, Y.-B., B. Dominic, S. Zani, M. T. Mellon, and J. P. Zehr.** 1999. Expression of photosynthesis genes in relation to nitrogen fixation in the diazotrophic filamentous nonheterocystous cyanobacterium *Trichodesmium* sp. IMS 101. Plant Mol. Biol. **41:**89–104.
6. **Church, M. J., C. M. Short, B. D. Jenkins, D. M. Karl, and J. P. Zehr.** 2005. Temporal patterns of nitrogenase gene (*nifH*) expression in the oligotrophic North Pacific Ocean. Appl. Environ. Microbiol. **71:**5362–5370.
7. **Colon-Lopez, M. S., D. M. Sherman, and L. A. Sherman.** 1997. Transcriptional and translational regulation of nitrogenase in light-dark- and continuous-light-grown cultures of the unicellular cyanobacterium *Cyanothece* sp. strain ATCC 51142. J. Bacteriol. **179:**4319–4327.
8. **Colon-Lopez, M. S., and L. A. Sherman.** 1998. Transcriptional and translational regulation of photosystem I and II genes in light-dark- and continuous-light-grown cultures of the unicellular cyanobacterium *Cyanothece* sp. strain ATCC 51142. J. Bacteriol. **180:**519–526.
9. **Curatti, L., P. W. Ludden, and L. M. Rubio.** 2006. NifB-dependent *in vitro* synthesis of the iron-molybdenum cofactor of nitrogenase. Proc. Natl. Acad. Sci. USA **103:**5297–5301.
10. **Fay, P.** 1992. Oxygen relations of nitrogen fixation in cyanobacteria. Microbiol. Rev. **56:**340–373.
11. **Florencio, F. J., M. E. Perez-Perez, L. Lopez-Maury, A. Mata-Cabana, and M. Lindahl.** 2006. The diversity and complexity of the cyanobacterial thioredoxin systems. Photosynth. Res. **89:**157–171.
12. **Gallon, J. R.** 1992. Reconciling the incompatible: N_2 fixation and O_2. New Phytol. **122:**571–609.
13. **Gallon, J. R., and A. E. Chaplin.** 1987. An introduction to nitrogen fixation. Cassell, London, England.
14. **Gallon, J. R., S. M. Perry, T. M. A. Rajab, K. A. M. Flayeh, J. S. Jones, and A. E. Chaplin.** 1988. Metabolic changes associated with the diurnal pattern of N_2-fixation in *Gloethece*. J. Gen. Microbiol. **134:**3079–3087.
15. **Garcia-Dominguez, M., M. I. Muro-Pastor, J. C. Reyes, and F. J. Florencio.** 2000. Light-dependent regulation of cyanobacterial phytochrome expression. J. Bacteriol. **182:**38–44.
16. **Gómez Casati, D. F., M. A. Aon, and A. A. Iglesias.** 2000. Kinetic and structural analysis of the ultrasensitive behaviour of cyanobacterial ADP-glucose pyrophosphorylase. Biochem. J. **350:**139–147.
17. **Haselkorn, R., and W. J. Buikema.** 1992. Nitrogen fixation in cyanobacteria, p. 166–190. *In* G. Stacey, R. H. Burris, and H. J. Evans (ed.), Biological nitrogen fixation. Chapman and Hall, New York, NY.
18. **Hernandez, J. A., R. Y. Igarashi, B. Soboh, L. Curatti, D. R. Dean, P. W. Ludden, and L. M. Rubio.** 2007. NifX and NifEN exchange NifB cofactor and the VK-cluster, a newly isolated intermediate of the iron-molybdenum cofactor biosynthetic pathway. Mol. Microbiol. **63:**177–192.
19. **Hu, Y., M. C. Corbett, A. W. Fay, J. A. Webber, K. O. Hodgson, and B. Hedman.** 2006. FeMo cofactor maturation on NifEN. Proc. Natl. Acad. Sci. USA **103:**17119–17124.
20. **Hu, Y., A. W. Fay, C. C. Lee, and M. W. Ribbe.** 2007. P-cluster maturation on nitrogenase MoFe protein. Proc. Natl. Acad. Sci. USA **104:**10424–10429.
21. **Huang, T., R. Lin, M. Chu, and H. Chen.** 1999. Organization and expression

of nitrogen-fixation genes in the aerobic nitrogen-fixing unicellular cyanobacterium *Synechococcus* sp. strain RF-1. Microbiology **145:**743–753.

22. **Huang, T. C., T. J. Chow, and I. S. Hwang.** 1988. The cyclic synthesis of the nitrogenase *Synechococcus* RF1 and its control at the transcriptional level. FEMS Microbiol. Lett. **50:**127–130.

23. **Jacobson, M. R., R. Premakumar, and P. E. Bishop.** 1986. Transcriptional regulation of nitrogen fixation by molybdenum in *Azotobacter vinelandii*. J. Bacteriol. **167:**480–486.

24. **Jakob, T., H. Wagner, K. Stehfest, and C. Wilhelm.** 2007. A complete energy balance from photons to new biomass reveals a light- and nutrient-dependent variability in the metabolic costs of carbon assimilation. J. Exp. Bot. **58:**2101–2112.

25. **Li, H., D. M. Sherman, S. Bao, and L. A. Sherman.** 2001. Pattern of cyanophycin accumulation in nitrogen-fixing and non-nitrogen-fixing cyanobacteria. Arch. Microbiol. **176:**9–18.

26. **Lindahl, M., and F. J. Florencio.** 2003. Thioredoxin-linked processes in cyanobacteria are as numerous as in chloroplasts, but targets are different. Proc. Natl. Acad. Sci. USA **100:**16107–16112.

27. **Lyons, E. M., and T. Thiel.** 1995. Characterization of *nifB*, *nifS*, and *nifU* genes in the cyanobacterium *Anabaena variabilis*: NifB is required for the vanadium-dependent nitrogenase. J. Bacteriol. **177:**1570–1575.

28. **Maier, R. J., and F. Moshiri.** 2000. Role of the *Azotobacter vinelandii* nitrogenase-protective Shethna protein in preventing oxygen-mediated cell death. J. Bacteriol. **182:**3854–3857.

29. **Moshiri, F., J. W. Kim, C. Fu, and R. J. Maier.** 1994. The FeSII protein of *Azotobacter vinelandii* is not essential for aerobic nitrogen fixation, but confers significant protection to oxygen-mediated inactivation of nitrogenase *in vitro* and *in vivo*. Mol. Microbiol. **14:**101–114.

30. **Mullineaux, P. M., J. R. Gallon, and A. E. Chaplin.** 1981. Acetylene reduction (nitrogen fixation) by cyanobacteria grown under alternating light dark cycles. FEMS Microbiol. Lett. **10:**245–247.

31. **Oelze, J.** 2000. Respiratory protection of nitrogenase in *Azotobacter* species: is a widely held hypothesis unequivocally supported by experimental evidence? FEMS Microbiol. Rev. **24:**321–333.

32. **Peschek, G. A., K. Villgrater, and M. Wastyn.** 1991. 'Respiratory protection' of the nitrogenase in dinitrogen-fixing cyanobacteria. Plant Soil **137:**17–24.

33. **Rabouille, S., M. Staal, L. J. Stal, and K. Soetaert.** 2006. Modeling the dynamic regulation of nitrogen fixation in the cyanobacterium *Trichodesmium* sp. Appl. Environ. Microbiol. **72:**3217–3227.

34. **Reddy, K. J., J. B. Haskell, D. M. Sherman, and L. A. Sherman.** 1993. Unicellular, aerobic nitrogen-fixing cyanobacteria of the genus *Cyanothece*. J. Bacteriol. **175:**1284–1292.

35. **Rees, D. C., F. Akif Tezcan, C. A. Haynes, M. Y. Walton, S. Andrade, O. Einsle, and J. B. Howard.** 2005. Structural basis of biological nitrogen fixation. Philos. Transact. A **363:**971–984.

36. **Rojek, R., C. Harms, M. Hebeler, and L. H. Grimme.** 1994. Cyclic variations of photosynthetic activity under nitrogen fixing conditions in *Synechococcus* RF-1. Arch. Microbiol. **162:**80–84.

37. **Scherer, S., H. Almon, and P. Böger.** 1988. Interaction of photosynthesis, respiration and nitrogen fixation in cyanobacteria. Photosynth. Res. **15:**95–114.

38. **Schneegurt, M. A., D. M. Sherman, S. Nayar, and L. A. Sherman.** 1994. Oscillating behavior of carbohydrate granule formation and dinitrogen fixation in the cyanobacterium *Cyanothece* sp. strain ATCC 51142. J. Bacteriol. **176:**1586–1597.

39. **Schneegurt, M. A., D. M. Sherman, and L. A. Sherman.** 1997. Composition of the carbohydrate granules of the cyanobacterium, Cyanothece sp. strain ATCC 51142. Arch. Microbiol. **167:**89–98.

40. **Schneegurt, M. A., D. M. Sherman, and L. A. Sherman.** 1997. Growth, physiology, and ultrastructure of a diazotrophic cyanobacterium, *Cyanothece* sp. strain ATCC 51142, in mixotrophic and chemoheterotrophic cultures. J. Phycol. **33:**632–642.

41. **Sherman, L. A., P. Meunier, and M. S. Colón-López.** 1998. Diurnal rhythms in metabolism: a day in the life of a unicellular, diazotrophic cyanobacterium. Photosynth. Res. **58:**25–42.

42. **Singh, A. K., H. Li, and L. A. Sherman.** 2004. Microarray analysis and redox control of gene expression in the cyanobacterium *Synechocystis* sp. PCC 6803. Physiol. Plant. **120:**27–35.

43. **Staal, M., S. Rabouille, and L. Stal.** 2007. On the role of oxygen for nitrogen fixation in the marine cyanobacterium *Trichodesmium* sp. Environ. Microbiol. **9:**727–736.

44. **Stal, L. J., and W. E. Krumbein.** 1985. Nitrogenase activity in the non-heterocyst cyanobacterium *Oscillatoria* sp. grown under alternating light-dark cycle. Microbiology **143:**67–71.

45. **Stal, L. J., and W. E. Krumbein.** 1987. Temporal separation of nitrogen fixation and photosynthesis in the filamentous, non-heterocystous cyanobacterium *Oscillatoria* sp. Arch. Microbiol. **149:**76–80.

46. **Stöckel, J., E. A. Welsh, M. Liberton, R. Kunnavakkan, and H. B. Pakrasi.** 2008. Global transcriptomic analysis of *Cyanothece* 51142 shows robust diurnal oscillation of central metabolic processes. Proc. Natl. Acad. Sci. USA **105:**6156–6161.

47. **Tezcan, F. A., J. T. Kaiser, D. Mustafi, M. Y. Walton, J. B. Howard, and D. C. Rees.** 2005. Nitrogenase complexes: multiple docking sites for a nucleotide switch protein. Science **309:**1377–1380.

48. **Tomitani, A., A. H. Knoll, C. M. Cavanaugh, and T. Ohno.** 2006. The evolutionary diversification of cyanobacteria: molecular-phylogenetic and paleontological perspectives. Proc. Natl. Acad. Sci. USA **103:**5442–5447.

49. **Ureta, A., and S. Nordlund.** 2002. Evidence for conformational protection of nitrogenase against oxygen in *Gluconacetobacter diazotrophicus* by a putative FeSII protein. J. Bacteriol. **184:**5805–5809.

50. **Valladares, A., I. Maldener, A. M. Muro-Pastor, E. Flores, and A. Herrero.** 2007. Heterocyst development and diazotrophic metabolism in terminal respiratory oxidase mutants of the cyanobacterium *Anabaena* sp. strain PCC 7120. J. Bacteriol. **189:**4425–4430.

51. **Wolk, C. P.** 1996. Heterocyst formation. Annu. Rev. Genet. **30:**59–78.

52. **Weng, J.-H., and Y.-J. Shieh.** 2004. Salicylhydroxamic acid (SHAM) inhibits O_2 photoreduction which protects nitrogenase activity in the cyanobacterium *Synechococcus* sp. RF-1. Photosynth. Res. **82:**151–164.

53. **Zehr, J. P., D. Harris, B. Dominic, and J. Salerno.** 1997. Structural analysis of the *Trichodesmium* nitrogenase iron protein: implications for aerobic nitrogen fixation activity. FEMS Microbiol. Lett. **153:**303–309.